**Title:** Muscimol hydration and vibrational spectroscopy – The impact of explicit and implicit water

**Author:** Piotr Najgebauer, Monika Staś, Roman Wrzalik, Małgorzata A. Broda, Piotr Paweł Wieczorek, Valery Andrushchenko, Teobald Kupka

**Citation style:** Najgebauer Piotr, Staś Monika, Wrzalik Roman, Broda Małgorzata A., Wieczorek Piotr Paweł, Andrushchenko Valery, Kupka Teobald. (2022). Muscimol hydration and vibrational spectroscopy – The impact of explicit and implicit water**.** "Journal of Molecular Liquids" (Vol. 363, (2022) art. no. 119870), doi 10.1016/j.molliq.2022.119870

Journal of Molecular Liquids 363 (2022) 119870

Contents lists available at ScienceDirect

Journal of Molecular Liquids

journal homepage: www.elsevier.com/locate/molliq

# Muscimol hydration and vibrational spectroscopy – The impact of explicit and implicit water

Piotr Najgebauer [a], Monika Staś [a,*], Roman Wrzalik [b,c], Małgorzata A. Broda [a], Piotr Paweł Wieczorek [a], Valery Andrushchenko [d,*], Teobald Kupka [a,*]

[a] Faculty of Chemistry, University of Opole, Oleska 48, 45-052 Opole, Poland
[b] A. Chełkowski Institute of Physics, University of Silesia, 75 Pułku Piechoty 1, 41-500 Chorzów, Poland
[c] Institute of Material Science, University of Silesia, 75 Pułku Piechoty 1a, 41-500 Chorzów, Poland
[d] Institute of Organic Chemistry and Biochemistry, Academy of Sciences, Flemingovo nám. 2, 16610 Prague, Czech Republic

ARTICLE INFO

*Article history:*
Received 24 April 2022
Revised 14 July 2022
Accepted 15 July 2022
Available online 20 July 2022

*Keywords:*
Molecular Dynamics (MD)
Muscimol
Density Functional Theory (DFT)
Tautomers
Hydrogen bonds
Hydration energy

ABSTRACT

The presented study focuses on the interaction of the well-known neurotoxin muscimol with water. Two approaches for the water solvent are applied – the explicit and the implicit. The muscimol-water clusters were obtained by the molecular dynamics simulations and the first solvation shell was kept for further studies. Implicit water was mimicked *via* the polarized continuum model (PCM). All three tautomeric forms of the free muscimol molecule are considered in the calculations. The combined theoretical and experimental vibrational IR and Raman studies determined the stability of the prevailing zwitterion form in water. We proved that water molecules in the first solvation shell are crucial for the correct prediction of structural and spectroscopic parameters of muscimol due to its ability to form strong hydrogen bonds. We believe that our findings will shed some light on the binding preferences of muscimol with the γ-aminobutyric acid (GABA) receptor.



## 1. Introduction

Muscimol is a heterocyclic neurotoxin [1] containing an isoxazole ring. It is produced by mushrooms of the genus *Amanita* and is a degradation product of ibotenic acid [2]. It was isolated in the 1960s by Japanese scientists [3,4], however, its psychoactive properties were well known long before and attracted great interest. For instance, mushrooms have been used by Siberian shamans [5]. Interestingly, muscimol is a conformational (rigidified) analogue of γ-aminobutyric acid (GABA) [6,7], and acts as an agonist of $GABA_A$ and $GABA_B$ receptors [8,9]. Moreover, it penetrates the blood–brain barrier [10]. Therefore, it was studied as a potential drug against Alzheimer's disease [11] and epilepsy [12]. Many reports in the area of neuroscience, pharmacology, toxicology, biochemistry, molecular biology and medicine which involved muscimol mainly acting as a $GABA_X$ receptor agonist have been published [13–18]. Despite this, surprisingly little is known about the chemistry of muscimol. In particular, limited studies involving theoretical chemistry approach were conducted to predict its properties [10,19–23].

Muscimol shows two pKa values (4.8 and 8.4), is soluble in water and can occur in three tautomeric forms (Fig. 1): **NH** (5-(aminomethyl)-1,2-oxazol-3-on), **OH** (5-(aminomethyl)-1,2-oxazol-3-ol) and **zwitterion** (5-(azaniumylmethyl)-1,2-oxazol-3-olate) [21]. Its zwitterionic structure has been determined by X-ray [24] and NMR studies [22]. Muscimol forms dimers held by strong intermolecular hydrogen bonds ($NH_3^+\cdots O^-$) in the crystal lattice. However, the studies on the structure and properties of muscimol mainly focused on one tautomeric form and only a limited number of discrete water molecules were used (if any) [7,10,19,21,22,24].

Although for many systems such an approach is sufficient, in this work we apply a different methodology. Considering the presence of heteroatoms with lone electron pairs in muscimol structure, accurate modelling of its direct interactions with polar solvent is very important [6]. Such an approach should better describe the interaction between muscimol tautomers and the surrounding polar solvent.

In this study, we performed fully unconstrained DFT optimizations of a free muscimol molecule in its three tautomeric forms and various environments and compared the results with its

* Corresponding authors.
*E-mail addresses:* 122217@student.uni.opole.pl (P. Najgebauer), mstas@uni.opole.pl (M. Staś), roman.wrzalik@us.edu.pl (R. Wrzalik), broda@uni.opole.pl (M.A. Broda), pwiecz@uni.opole.pl (P.P. Wieczorek), andrushchenko@uochb.cas.cz (V. Andrushchenko), teobaldk@gmail.com (T. Kupka).

https://doi.org/10.1016/j.molliq.2022.119870
0167-7322/

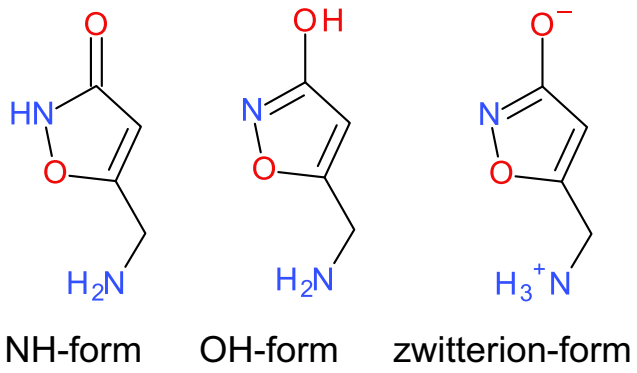


**Fig. 1.** Chemical structures of three tautomeric forms of muscimol.

hydrated analogues, obtained from molecular dynamics (MD) simulations. The main objective of this paper is to describe the impact of the implicit and explicit water solvent on muscimol structure and its IR/Raman spectroscopic parameters. Additionally, an effect of empirical dispersion correction (GD3) [25] on the computed results has been assessed.

## 2. Experimental part and theoretical methodology

### 2.1. Computational details

#### 2.1.1. DFT calculations

DFT calculations were performed using Gaussian 16 program package [26]. The initial structures of tautomers were prepared with GaussView 5 [27]. Calculations were done for three tautomeric forms of muscimol (**NH**, **OH** and **zwitterion**) in the gas phase, and in three solvents - chloroform, DMSO, and water. The solvent effect was simulated with the standard PCM approach [28], as well as using the explicit solvent molecules. Optimizations were performed utilizing the efficient hybrid B3LYP density functional [29,30] and a fairly large and flexible aug-cc-pVTZ basis set. Very tight optimization criteria and a large grid were used. In some calculations, dispersion effects were included using the empirical Grimme's D3 correction term [25]. Unconstrained optimizations were followed by vibrational analysis to ensure that the resulting structures are true energy minima, and the IR and Raman spectra were calculated. Complexation energies were determined utilizing the counterpoise [31] method, treating all solvent molecules as a single molecule.

#### 2.1.2. MD simulations

A molecular dynamic simulation was set up for the studied tautomers under the periodic boundary conditions; 10 ns simulation run at 300 K and pressure 1 atm. The starting geometries of the tautomers were obtained after the gas-phase DFT optimization of the GaussView-generated structures, as described in the previous section. The compounds were solvated in a periodic rectangular box with a 12 Å cut-off, filled with 861, 869 and 841 TIP3P water molecules for **NH**, **OH** and **zwitterion** tautomers, respectively, using TLeap [32]. The box dimensions for the three tautomers after the equilibration were $31.0 \times 30.3 \times 28.2$ Å$^3$, $30.0 \times 31.5 \times 28.1$ Å$^3$ and $31.6 \times 29.3 \times 27.5$ Å$^3$, respectively. The MD simulations were done with AMBER14 [32] using the supplied general amber force field (GAFF) for the studied molecules and the "ff14SB" force field for water. Atomic charges were obtained from the R.E.D. Server Development software [33–35]. After a sequence of restrained minimizations for 8000 steps with a combination of steepest descent and conjugate gradient algorithms and heating for 20 ps with NVT ensemble, 100 ps equilibration dynamics was performed at 300 K without any restraints. The equilibration and production runs were performed with NPT ensemble, the temperature was controlled by Langevin thermostat (collision frequency of 1 ps$^{-1}$) and isotropic position scaling was used with Berendsen barostat to control the average pressure at 1 atm. The SHAKE algorithm was used with a tolerance of $10^{-5}$ Å and 2 fs integration time step. The Lennard-Jones interactions were cut-off at 10 Å. To account for the long-range electrostatic interactions, the particle mesh Ewald method (PME) was employed. Considering a relatively small and simple system, 100 ps equilibration time was sufficient, as confirmed by the time evolution of the total potential energy (EPtot) and density of the simulated systems in Figs. S1–S3 of the Supporting Information (SI).

#### 2.1.3. Additional computational analysis

A set of 200 equidistant snapshots was selected from the 10 ns production MD trajectory (one snapshot every 50 ps, to ensure their independence). For each selected snapshot, the water molecules outside of the first hydration shell were truncated with the "xshell" program [36] using the cut-off parameter of 2.5 Å. The program keeps the water molecules with at least one atom located within 2.5 Å from the solute while removing the rest of the water molecules. The cut-off parameter was determined from the radial distribution function (RDF) plots using the "rdf" program [37] and was the same for all the studied systems (Fig. S4 in SI). The number of water molecules in the first hydration shell for each of the 200 selected snapshots was automatically provided by the "xshell" program.

For each tautomer, a snapshot with the most relevant number of water molecules in the first hydration shell was selected and subjected to further full DFT optimization at B3LYP/aug-cc-pVTZ level of theory, both in the gas phase and with PCM/water implicit solvent. Vibrational IR and Raman spectra were computed for the snapshots. The scaling factor of 0.968 for harmonic frequencies was taken from Computational Chemistry Comparison and Benchmark DataBase [38]. To assess the accuracy of the resulting theoretical structures of muscimol, deviations between the calculated and the experimental (obtained from X-ray structure [24]) bond lengths (Theor. – Exp.), as well as their root-mean-square deviation (RMSD) were calculated.

#### 2.1.4. Experimental details

***FTIR spectra:*** An FT-IR spectrometer Nicolet iS50 (Thermo Fisher Scientific, USA) equipped with the attenuated total reflection (ATR) diamond accessory MIRacle (PIKE Technology, USA) was used for the measurements. 64 scans were accumulated with 2 cm$^{-1}$ resolution (spectral resolution 0.482 cm$^{-1}$) in the spectral range 400–4000 cm$^{-1}$. ATR correction was used to transform the reflectance spectrum to a log (1/R) absorption spectrum (muscimol refractive index is 1.45).

***Raman spectra:*** An alpha300R confocal Raman microscope (WITec, Germany) was used to measure spectra of dried muscimol crystals. The spectra were acquired 100 times in the ranges from 180 to 4000 cm$^{-1}$ with a 2 cm$^{-1}$ spectral resolution (diffraction grating 600 lines / millimeter) and 500–1630 cm$^{-1}$ with a spectral resolution of 1 cm$^{-1}$ (grating 1800 lines / millimeter). The incident 532 nm laser beam with a power of 1 mW was focused on the sample surface using the FLPlanFl 50x/0.5 objective (Olympus, Japan).

## 3. Results and discussion

### 3.1. Structure and hydration of muscimol molecule

To adequately describe the muscimol properties, the models of muscimol tautomers for free molecules were created, followed by

muscimol-water clusters generated from the MD simulation. Free muscimol tautomers were optimized in the gas phase and in three environments of different polarity including chloroform, DMSO, and water. Even though muscimol is not soluble in chloroform, this solvent was selected to observe hypothetical weak interactions with the solvent [21]. The unconstrained optimized structures of muscimol tautomers with atom numbering are shown in Fig. 2.

To obtain the muscimol-water clusters, we used molecular dynamics simulations to estimate the number of water molecules in the first solvation shell [39,40]. We determined the extent of the first hydration shell to be 2.5 Å based on the RDF plots (Fig. S4). Larger cut-offs resulted in the inclusion of waters from the second hydration shell, which were not hydrogen-bonded with the solute but only with each other, thus not affecting the geometry and the vibrational properties/spectra of the solute significantly. Therefore, the water molecules located at distances further than 2.5 Å from the solute were not considered. The obtained truncated MD snapshot clusters were optimized in the gas phase and implicit water.

The MD results show that the number of water molecules around the muscimol varies for the studied tautomers (Fig. 3). Around 25 % of **NH**-form molecules are surrounded by seven water molecules and around 20 % by six water molecules. The mean of the number of water molecules distribution is 6.0. In the **OH**-form almost 25 % of molecules are interacting with six water molecules. The mean of the distribution is 5.6, somewhat smaller than for **NH**-form. On the other hand, more than 20 % of **zwitterion**-form is hydrated by nine water molecules and the mean distribution is almost two units higher and equals 8.1. The larger number of the waters solvating the zwitterionic form can be explained by the presence of two charged tails which attract more water molecules and create stronger interactions. Fig. 4 shows the arrangement of water molecules in the first hydration sphere for the three tautomers. It is apparent that the **zwitterion** has a higher number of hydrogen bonds binding solvent molecules than other tautomers (7 *vs* 5). Interestingly, although water molecules create hydrogen bonds with the heteroatoms of the solute, the interaction with the etheric oxygen in the ring is very rare among the cluster population (not shown). Some of the water molecules, while being in the first hydration shell, do not form hydrogen bonds with the solute but rather interact only with each other.

The bond length deviations between the calculated and the experimental data [24] for three tautomeric forms of free muscimol and its hydrates in various environments are gathered in Table 1. The corresponding bond lengths are provided in Tables S1–S3 in the SI.

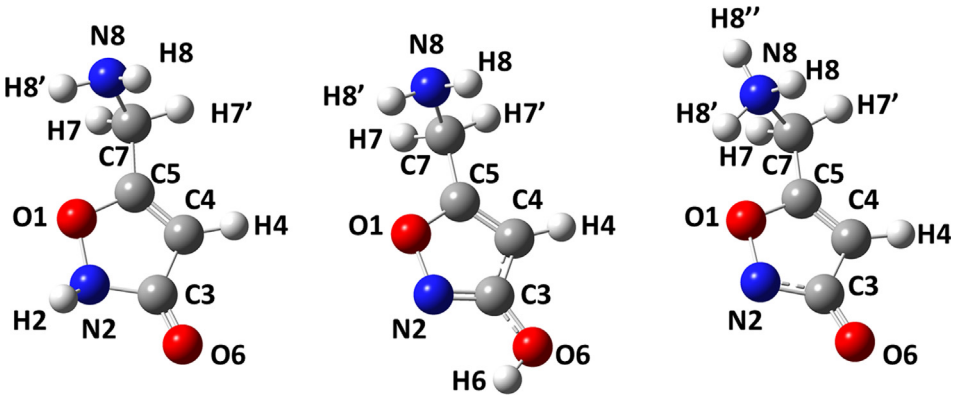


**Fig. 2.** Three optimized (B3LYP/aug-cc-pVTZ) tautomeric forms of muscimol with atom numbering: **NH**, **OH**, and **zwitterion**.

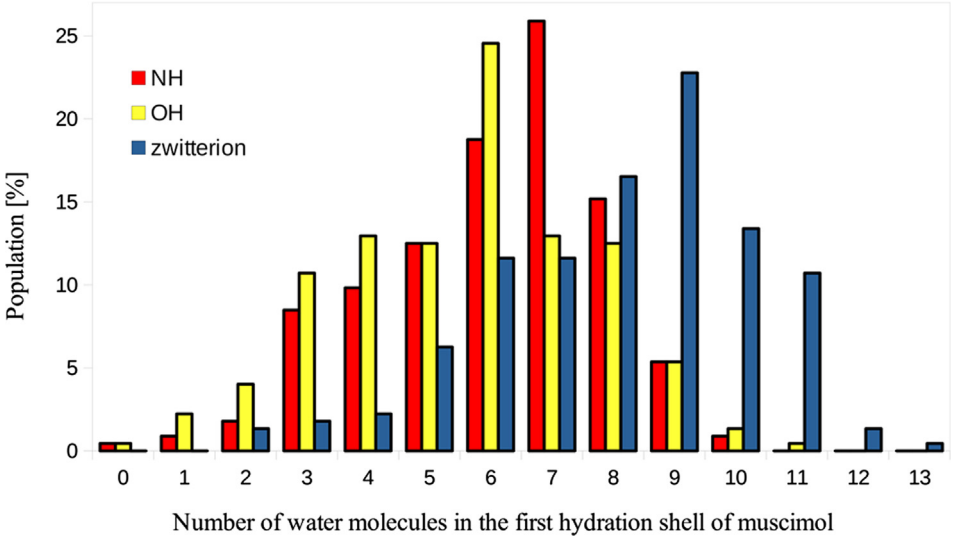


**Fig. 3.** The number of water molecules in the first hydration shell of three muscimol tautomers derived from the MD simulations (distance up to 2.5 Å, results from MD with GAFF force field).

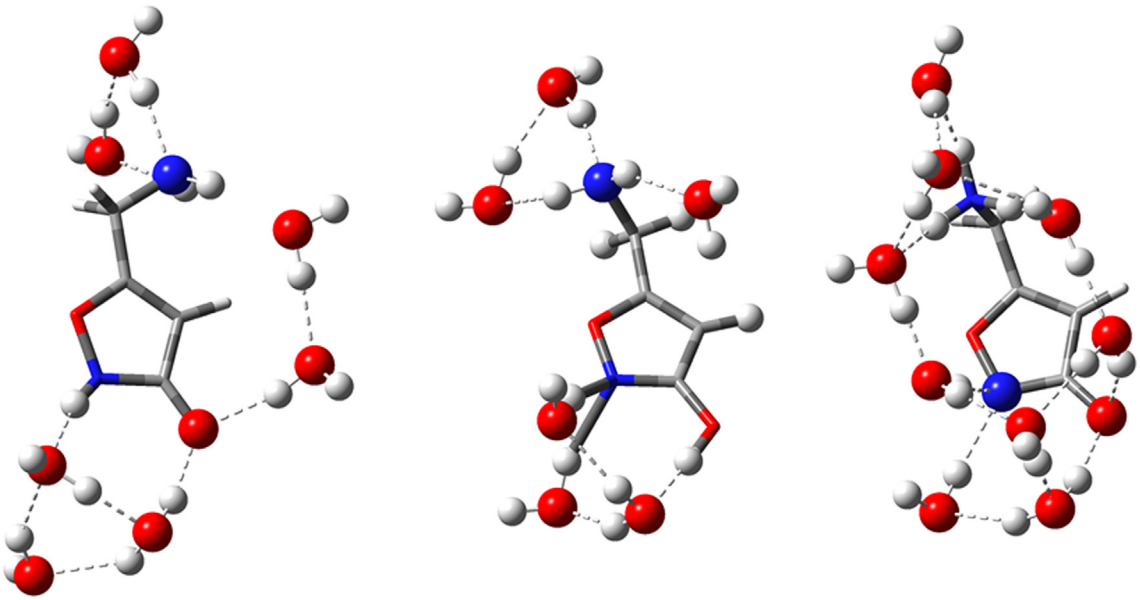

**Fig. 4.** Optimized (B3LYP/aug-cc-pVTZ) structures of **NH**, **OH**, and **zwitterion** tautomers of muscimol clusters with the most prevalent number of water molecules (7, 6, and 9) derived from the MD simulation.

The smallest deviation from the crystal structure occurs for the **OH**-form both for the free molecule (RMSD = 0.0205 Å) and its hydrate (RMSD = 0.0370 Å). The biggest differences are predicted for the hydrated NH-form in the gas phase (RMSD = 0.0885 Å) *vs* water (RMSD = 0.0432 Å). Considerable differences in RMSD values can be noticed for gas-to-solvents shifts, especially for the **zwitterion**, (from 0.0424 in the gas phase to 0.0287 Å in chloroform.) Altering the environment from chloroform to water or DMSO has not caused significant deviations in the bond lengths, moreover, the difference in RMSD is very small for all tautomeric forms in polar solvents. Another big change in the bond length is caused by the explicit water molecules for all forms, especially for the **NH**-form (RMSD change from 0.0503 to 0.0885 Å). Interestingly, the bond lengths measured for clusters with an additionally applied PCM-SCRF solvent model have a little smaller RMSD than clusters in the gas phase, except for the **zwitterion**.

Fig. 5 shows the bond lengths for all tautomeric forms with explicit and implicit water. It is apparent that the PCM method

**Table 1**
RMSD of B3LYP-D3/aug-cc-pVTZ calculated bond lengths (in Å) from X-ray experiment [24] for free muscimol tautomers and their hydrates in various environments.

| Bond | Gas phase | $CHCl_3$ | DMSO | Water | Hydrate gas phase | Hydrate PCM water |
|---|---|---|---|---|---|---|
| | | | | *NH form* | | |
| C3C4 | 0.0185 | 0.0127 | 0.0102 | 0.0100 | 0.0016 | 0.0005 |
| C4C5 | −0.0011 | 0.0011 | 0.0020 | 0.0021 | 0.0010 | 0.0015 |
| C5C7 | 0.0068 | 0.0064 | 0.0062 | 0.0062 | 0.0041 | 0.0043 |
| C3O6 | −0.0905 | −0.0812 | −0.0772 | −0.0770 | −0.0577 | −0.0539 |
| C5O1 | 0.0041 | 0.0028 | 0.0019 | 0.0018 | 0.0008 | −0.0008 |
| C3N2 | 0.1036 | 0.0927 | 0.0888 | 0.0886 | 0.0576 | 0.0539 |
| C7N8 | −0.0297 | −0.0853 | −0.0272 | −0.0271 | −0.0328 | −0.0309 |
| O1N2 | −0.0079 | −0.0132 | −0.0153 | −0.0154 | −0.0242 | −0.0260 |
| **RMSD** | **0.0503** | **0.0534** | **0.0433** | **0.0432** | **0.0885** | **0.0829** |
| | | | | *OH form* | | |
| C3C4 | −0.0167 | −0.0171 | −0.0173 | −0.0174 | −0.0114 | −0.0147 |
| C4C5 | 0.0112 | 0.0106 | 0.0103 | 0.0103 | 0.0125 | 0.0107 |
| C5C7 | 0.0061 | 0.0059 | 0.0057 | 0.0057 | 0.0060 | 0.0041 |
| C3O6 | 0.0411 | 0.0395 | 0.0388 | 0.0388 | 0.0104 | 0.0171 |
| C5O1 | −0.0082 | −0.0064 | −0.0055 | −0.0055 | −0.0132 | −0.0093 |
| C3N2 | −0.0077 | −0.0057 | −0.0049 | −0.0048 | 0.0103 | 0.0089 |
| C7N8 | −0.0273 | −0.0253 | −0.0242 | −0.0242 | −0.0251 | −0.0209 |
| O1N2 | −0.0190 | −0.0164 | −0.0153 | −0.0152 | −0.0132 | −0.0147 |
| **RMSD** | **0.0205** | **0.0193** | **0.0188** | **0.0187** | **0.0370** | **0.0356** |
| | | | | *Zwitterion form* | | |
| C3C4 | 0.0533 | 0.0351 | 0.0281 | 0.0278 | 0.0098 | 0.0191 |
| C4C5 | −0.0088 | −0.0046 | −0.0027 | −0.0026 | −0.0014 | −0.0042 |
| C5C7 | −0.0125 | −0.0085 | −0.0069 | −0.0068 | −0.0021 | −0.0039 |
| C3O6 | −0.0663 | −0.0463 | −0.0384 | −0.0380 | −0.0289 | −0.0419 |
| C5O1 | −0.0026 | −0.0088 | −0.0084 | −0.0083 | −0.0071 | −0.0086 |
| C3N2 | 0.0506 | 0.0395 | 0.0361 | 0.0359 | 0.0326 | 0.0376 |
| C7N8 | 0.0515 | 0.0308 | 0.0254 | 0.0251 | 0.0062 | 0.0073 |
| O1N2 | 0.0414 | 0.0234 | 0.0167 | 0.0164 | 0.0017 | 0.0085 |
| **RMSD** | **0.0424** | **0.0287** | **0.0240** | **0.0238** | **0.0457** | **0.0609** |

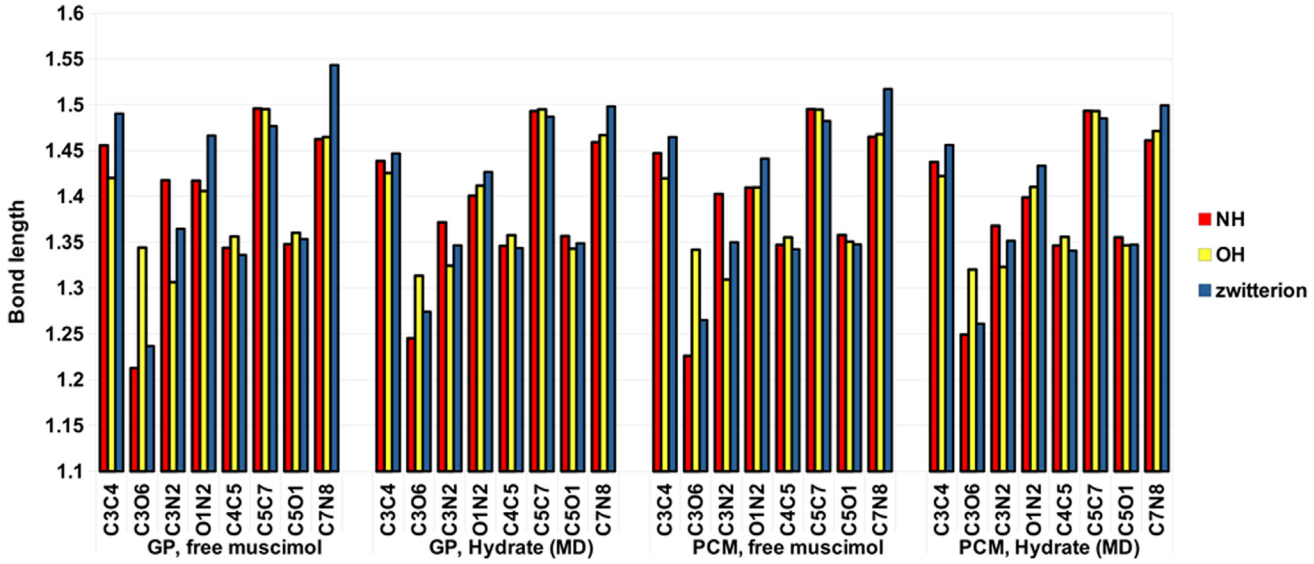


**Fig. 5.** Selected bond lengths of free muscimol tautomers and their MD-generated clusters with water calculated in the gas phase (GP) and in PCM water solvent. Only clusters with the most prevalent hydration number were considered.

**Table 2**
B3LYP/aug-cc-pVTZ stabilization energy (in kcal/mol) of muscimol tautomers in various environments with and without the inclusion of dispersion correction.

| | No D3 | | | With D3 | | |
|---|---|---|---|---|---|---|
| | NH | OH | zwitterion | NH | OH | zwitterion |
| Gas phase | 1.87 | 0.00 | 51.87 | 1.45 | 0.00 | 51.63 |
| PCM/Chloroform | 0.09 | 0.00 | 22.84 | 0.00 | 0.33 | 22.82 |
| PCM/DMSO | 0.00 | 0.65 | 12.03 | 0.00 | 1.06 | 12.17 |
| PCM/Water | 0.00 | 0.69 | 11.49 | 0.00 | 1.09 | 11.64 |

**Table 3**
B3LYP-D3/aug-cc-pVTZ stabilization energies (in kcal/mol) of muscimol tautomers with six water molecules in the first hydration shell.

| | NH cluster | OH cluster | Zwitterion cluster |
|---|---|---|---|
| Gas phase | 0.00 | 2.44 | 31.55 |
| PCM/Water | 1.85 | 2.28 | 0.00 |

shortens them. Besides, the impact of solvation depends on the bond type. For example, the bond length of the double bond (C4=C5) remains almost unchanged but the C3N2 and C3O6 bonds change irregularly depending on the tautomer and method of solvent treatment.

The inclusion of dispersion correction does not influence the structural parameters by more than 2% (Tables S1–S3). This may confirm that the intermolecular hydrogen bonds and not the Van der Waals or London interactions are the main stabilizing forces for muscimol monomeric structure in solution. Therefore, the inclusion of explicit water can be crucial to correctly model muscimol properties.

However, it must be kept in mind that muscimol occurs as a **zwitterion** in the crystalline state and forms dimers, where the oppositely charged groups interact with each other [24]. In solution, on the other hand, muscimol interacts with several solvent molecules by H-bonds which are more relaxed and longer than in the crystal.

### 3.2. Energies

Knowing the probable structures of muscimol, we could proceed to estimate the energy of the tautomers in various environments. Table 2 summarizes the stabilization energies of three muscimol tautomers in the gas phase, chloroform, DMSO, and water. The results show that the most stable forms in the gas phase and in the selected solvents are **NH** and **OH**. However, in contrast to **OH**, the **NH** form is stabilized with the increased solvent polarity. The least stable is the **zwitterion** and its energy in the gas phase is about 52 kcal/mol higher than that of the **OH** form. Similarly, the **zwitterion** is the least stable in chloroform and polar solvent (by about 23 and 12 kcal/mol). The inclusion of dispersion correction does not influence the results. These results are in contrast to the experimental data which confirmed the presence of **zwitterion** both in solution [22] and in the crystalline state [24].

**Table 4**
B3LYP-D3/aug-cc-pVTZ calculated complexation energies (in kcal/mol) of muscimol hydrates for the most prevalent solvation number in the gas phase.

| Cluster | $\Delta E_{comp}$ | Number of water molecules | $\Delta E_{comp}$/water molecule | $\Delta E_{comp}$/hydrogen bond |
|---|---|---|---|---|
| NH | 47.71 | 7 | 6.82 | 9.54 |
| OH | 46.92 | 6 | 7.82 | 9.38 |
| Zwitterion | 112.95 | 9 | 12.55 | 16.14 |

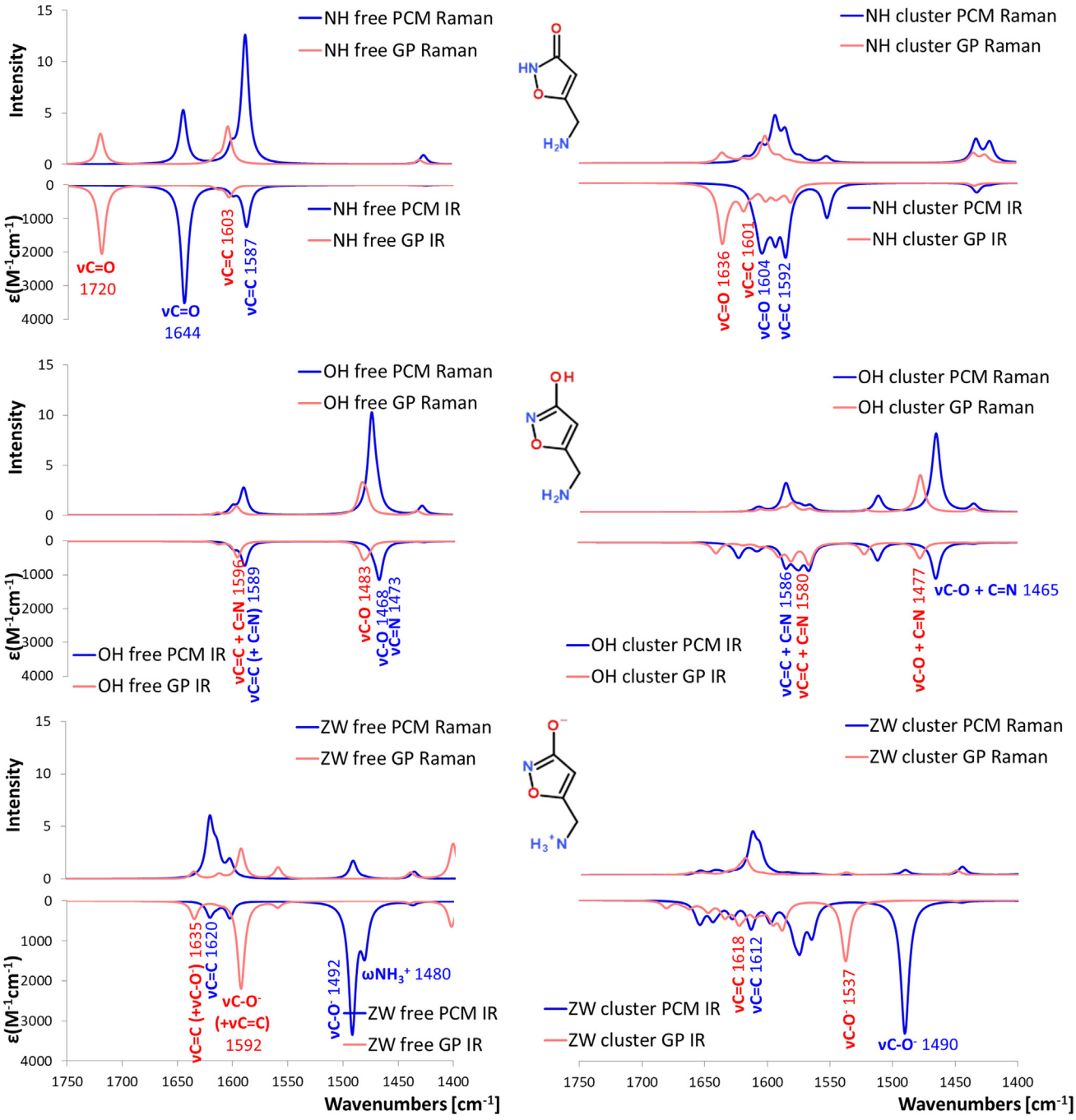


**Fig. 6.** Theoretical IR (downward curves) and Raman (upward curves) spectra of **NH**, **OH** and **zwitterion** tautomeric forms of free muscimol and their water clusters calculated at B3LYP/aug-cc-pVTZ level of theory in the gas phase (GP) and with PCM/water (PCM) using a scaling factor of 0.968 [38]. ε stands for the molar absorption coefficient.

This inconsistency was tackled by including the water molecules of the first solvation shell obtained from the MD simulations. The energy of the tautomers with an equal number of water molecules (six) was calculated in the gas phase and with additional implicit water modelled by PCM. As the result, in the gas phase, the **zwitterion** hydrate energy was still higher by 31.55 kcal/mol than the lowest energy **NH** hydrate. However, additional implicit water, representing the long-range bulk polar solvent, substantially decreased the **zwitterion** energy, making it the lowest energy tautomer in the implicit solvent (by about 2 kcal/mol lower than the other tautomers, Table 3).

Apart from the tautomers' relative energy, the water complexation energy was estimated. These data are presented in Table 4. The water-muscimol clusters have different number of water molecules so the energy was recalculated per water molecule and hydrogen bond. The highest complexation energy has the **zwitterion** - almost twice as high as the other tautomers. This high energy gain can be caused by the electrostatic interaction between the charged tails of the **zwitterion**. As expected, the hydrogen bonds created by the $NH_3^+$ group are shorter (and stronger) than the bonds made by the $NH_2$ group (Table S4).

### 3.3. Calculated and experimental IR and Raman spectra

Infrared and Raman spectra were calculated for all tautomeric forms of free muscimol and their clusters with water molecules,

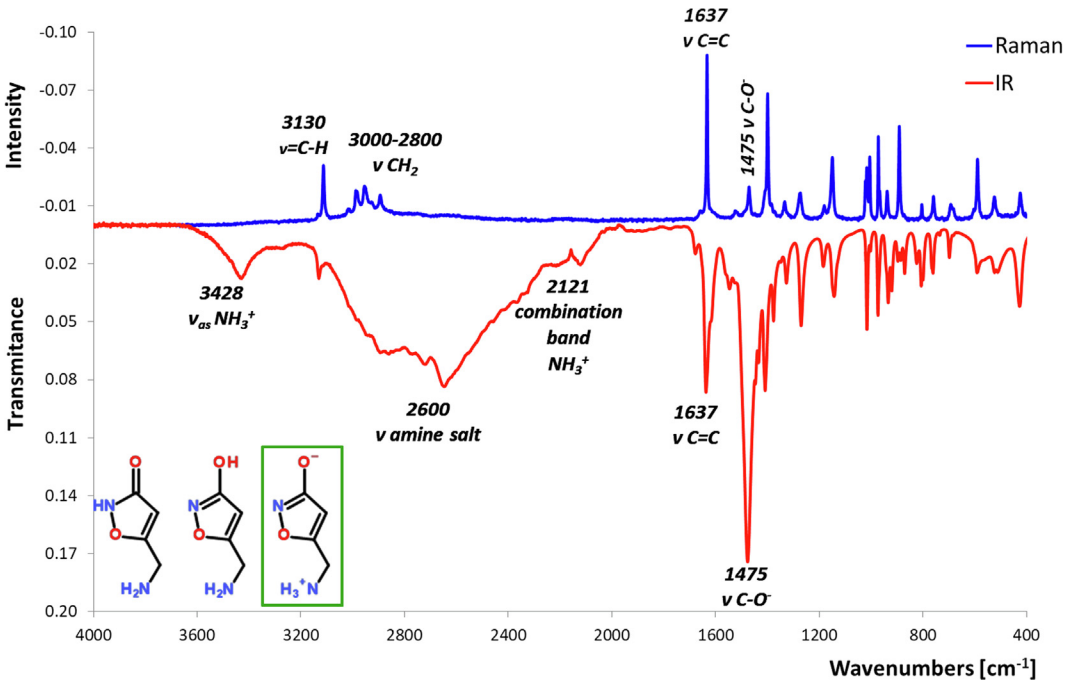


**Fig. 7.** Experimental Raman (upward curve, blue line) and ATR-IR (downward curve, red line) spectra of solid muscimol (Raman intensities were multiplied by −0.01).

both in the gas phase and with implicit PCM water. The most distinctive structural difference between the muscimol tautomers is due to the presence (or lack) of the carbonyl and imine groups. The corresponding stretching vibrations are visible in the predicted IR and Raman spectra in the range from 1750 to 1400 $cm^{-1}$. The C═C stretching vibration is also observed for all tautomers. Fig. 6 shows the theoretical IR and Raman spectra of the studied tautomers in the spectral range 1750–1400 $cm^{-1}$, the entire range spectra are shown in Fig. S5 in SI. The presence of water, modelled by implicit and explicit solvent, as well as the long-range bulk solvent effect, results in noticeable redshifts of muscimol bands (up to 100 $cm^{-1}$ in the case of νC-$O^-$, Fig. 6). For muscimol explicitly solvated by several water molecules, crowded spectra containing slightly different $\nu_{OH(sym)}$ and $\nu_{OH(asym)}$ vibrations of the explicit water molecule are calculated. Significant redshifts of $\nu_{C=O}$ and $\nu_{OH}$ bands are observed as a result of the water molecules interacting with the solute and forming strong (very short) hydrogen bonds with these groups. The most significant shift toward lower wavenumbers is observed for the $\nu_{C=O}$ band of **NH** form (for details see Tables S5–S7). On the other hand, the smallest impact of the solvent is predicted both for the explicit and implicit models in the calculated spectra of hydrated **OH** tautomer. This could be because water interacts stronger with substituents than with the isoxazole ring. The C═O and C═N stretching vibrations are coupled in the free **OH** form both in the gas phase and in PCM/water calculations, while the C═C and C—$O^-$ vibrations are coupled in the free **zwitterion** only in the gas phase. Different effect of the implicit and explicit solvent on the spectra of different tautomers can be seen in Fig. 6. Thus, the $\nu_{C=O}$ wavenumber of the free **NH** form calculated in the gas phase shifts down by 84 $cm^{-1}$ from 1720 to 1636 $cm^{-1}$ due to accounting for the explicit water molecules alone, while the shift due to the implicit PCM solvent is somewhat lower (76 $cm^{-1}$). Possibly, this could be connected with the high sensitivity of the carbonyl group in the **NH** tautomer to hydrogen bonding represented by the explicit water model. On the other hand, the large shift of the $\nu_{C-O}^-$ anion in the **zwitterion**, strongly affected by the electrostatic interactions, is well modelled already by the implicit solvent, reaching 100 $cm^{-1}$ (from 1592 to 1492 $cm^{-1}$), and providing almost the same value as the combination of the two solvent models (102 $cm^{-1}$). This emphasizes the importance of accounting for both implicit and explicit solvent, particularly in the calculations of sensitive to interactions vibrational spectra.

Only fragments of experimental IR spectra of muscimol were reported in the 1980s [41–43], while, according to our best knowledge, no Raman spectra are available.

ATR-IR and Raman spectra of muscimol are presented in Fig. 7 in the range from 4000 to 400 $cm^{-1}$. The tentative spectral band assignments are provided based on our B3LYP/aug-cc-pVTZ calculations.

The IR spectrum of solid muscimol in Fig. 7 is dominated by wide bands characteristic of the –$NH_3^+$ group. Furthermore, a comparison with the calculated spectra of all tautomers suggests that the IR spectra of the **zwitterion** form agree the most with the experiment. Thus, the strongest IR band at 1475 $cm^{-1}$ in the experiment can be assigned to the calculated at 1490 $cm^{-1}$ $\nu_{C-O}^-$ band, while the lower intensity band at 1637 $cm^{-1}$ could be most probably attributed to the multiple computed bands around 1620 $cm^{-1}$. Note that calculated IR spectra of the other tautomers do not feature the strongest band around 1480–1490 $cm^{-1}$, observed in the experiment. Moreover, no bands which could be undoubtedly identified with either carboxyl or hydroxyl group appear in the experimental spectrum, in concert with the computed zwitterion spectrum. Therefore, we could assume the presence of **zwitterion** form in the solid-state samples, in accord with the earlier X-ray studies [24]. It is worth mentioning that only the zwitterion spectra calculated with the inclusion of the water (either implicit or a combination of the implicit and explicit) result in faithful agreement with the experiment (cf. Figs. 6 and 7). The gas-phase spectra show a much poorer resemblance with the experimental spectra and could not be used for reliable band assignments.

The broad band at 3428 $cm^{-1}$ could originate from the asymmetric stretching mode of the —$NH_3^+$ group [44]. The IR absorption region 3200–2400 $cm^{-1}$ is characterized by broad bands with multiple peaks due to symmetric stretching modes of hydrogen-

bonded $-NH_3^+$ groups. The band at 2121 $cm^{-1}$ is assigned to the combination of asymmetric bending and torsion of $-NH_3^+$ modes. In the Raman spectrum, the region 3200–2800 $cm^{-1}$ is dominated by C—H and $CH_2$ modes. The Raman band at 1475 $cm^{-1}$, as suggested by the calculations, is assigned to the stretching vibration of the $C-O^-$ group, while the most intense peak at 1637 $cm^{-1}$ comes mainly from the stretching vibration of the C=C bond.

The spectral assignments presented above are consistent with the scarce IR data available for muscimol [41–43]. Our IR/Raman results support the presence of the **zwitterion** form of muscimol in the solid-state, as suggested by the results of X-ray studies [24]. Moreover, our theoretical DFT analysis suggests the presence of the **zwitterion** form in water, in agreement with the experimental NMR solution studies [22].

## 4. Conclusions

In the current study, we analysed the structure, energy and vibrational properties of three tautomeric forms of muscimol in solvents treated as explicit and implicit models. Theoretical DFT calculations were combined with MD simulations of explicit water molecules in the first hydration shell of muscimol. Experimental vibrational IR/Raman studies of solid muscimol were also measured and the resulting spectra were assigned with the help of the calculations.

Based on our DFT and MD calculations, the zwitterion tautomer was selected as the most stable form of muscimol in water. It was essential to include both explicit and implicit solvents together to correctly predict the energetically most stable tautomer of muscimol in water. For the first time, the entire IR/Raman spectrum of solid muscimol was reported and its zwitterion form in the solid-state was confirmed.

The predicted vibrational spectra of muscimol were sensitive to the presence of water and in comparison to the gas phase results, a significant red shift of characteristic peaks was observed. Thus, the spectra calculated with a water model (both implicit and explicit) showed significantly better agreement with the experimental spectra and much closer positions of the main spectral bands to those in the experiment. Furthermore, the absence of carbonyl and hydroxyl group IR signal in the solid-state experimental spectra was demonstrated by the calculated spectra of the zwitterion form of muscimol, confirming prevalence of this tautomer in the solid-state.

The obtained results point out the importance of both explicit and implicit solvent treatment for proper modelling of medium size molecules in solution.

## Data availability

Data will be made available on request.

## Declaration of Competing Interest

The authors declare that they have no known competing financial interests or personal relationships that could have appeared to influence the work reported in this paper.

## Acknowledgement

Calculations have been carried out using resources provided by Wroclaw Centre for Networking and Supercomputing (https://wcss.pl). Some of us are grateful for a partial support from the Faculty of Chemistry, University of Opole. The work was in part supported from European Regional Development Fund; OP RDE; Project: "ChemBioDrug" (No. CZ.02.1.01/0.0/0.0/16_019/0000729).

## Appendix A. Supplementary material

Supplementary data to this article can be found online at https://doi.org/10.1016/j.molliq.2022.119870.

## References

[1] E. Flament, J. Guitton, J.-M. Gaulier, Y. Gaillard, Pharmaceuticals 13 (2020) 454.
[2] A. Poliwoda, K. Zielińska, M. Halama, P.P. Wieczorek, Electrophoresis 35 (2014) 2593.
[3] M. Onda, H. Fukushima, M. Akagawa, Chem. Pharm. Bull. 12 (1964) 751.
[4] R. Good, G.F.R. Müller, C.H. Eugster, Helv. Chim. Acta 48 (1965) 927.
[5] M.R. Lee, E. Dukan, I. Milne, J.R. Coll, Physicians Edinb. 48 (2018) 85.
[6] T. Boulanger, D.P. Vercauteren, F. Durant, J.-M. Andre, Int. J. Quantum Chem. 34 (1988) 149.
[7] E. Gálvez-Ruano, I. Iriepa, A. Morreale, D.B. Boyd, J. Mol. Graphics Modell. 20 (2001) 183.
[8] G.A. Johnston, Neurochem. Res. 39 (2014) 1942.
[9] L. Brehm, H. Hjeds, P. Krogsgaard-Larsen, Acta Chem. Scand. 26 (1972) 1298.
[10] G. Serdaroğlu, Int. J. Quantum Chem. 111 (2010) 3938.
[11] V. Pilipenko, K. Narbute, U. Beitnere, J. Rumaks, J. Pupure, B. Jansone, V. Klusa, Eur. J. Pharmacol. 818 (2018) 381.
[12] J.D. Heiss, D.P. Argersinger, W.H. Theodore, J.A. Butman, S. Sato, O.I. Khan, Neurosurgery 85 (2019) E4.
[13] L.L. Wellman, G. Lonart, A.M. Adkins, L.D. Sanford, Brain Res. 1781 (2022) 147816.
[14] H.N. Carlson, B.A. Christensen, W.E. Pratt, Neurosci. Lett. 771 (2022) 136417.
[15] N.S. Rieger, N.B. Worley, A.J. Ng, J.P. Christianson, Behav. Brain Res. 416 (2022) 113541.
[16] R.A. Costa, Z. Velez, P.C. Hubbard, J. Exp. Biol. 225 (2022) jeb243112.
[17] J.L. Giacomini, K. Sadeghian, B.A. Baldo, Neuropsychopharmacology 47 (2022) 1358.
[18] A.B. de Landeta, M. Pereyra, M. Miranda, P. Bekinschtein, J.H. Medina, C. Katche, Neurobiol. Learn. Mem. 186 (2021) 107544.
[19] G. Serdaroğlu, Indian J. Chem., Sect A 56 (2017) 1143.
[20] F. Kiani, M. Abbaszadeh, M. Pousti, F. Koohyar, Braz. J. Pharm. Sci. 51 (2015) 213.
[21] T. Kupka, P.P. Wieczorek, Spectrochim. Acta A Mol. Biomol. Spectrosc. 153 (2016) 216.
[22] T. Kupka, M.A. Broda, P.P. Wieczorek, Magn. Reson. Chem. 58 (2020) 584.
[23] M. Ramek, P.I. Nagy, J. Phys. Chem. A 104 (2000) 6844.
[24] L. Brehm, K. Frydenvang, L.M. Hansen, P.O. Norrby, P. Krogsgaard-Larsen, T. Liljefors, Struct. Chem. 8 (1997) 443.
[25] S. Grimme, J. Antony, S. Ehrlich, H. Krieg, J. Chem. Phys. 132 (2010) 154104.
[26] M. J. Frisch, G. W. Trucks, H. B. Schlegel, G. E. Scuseria, M. A. Robb, J. R. Cheeseman, G. Scalmani, V. Barone, G. A. Petersson, H. Nakatsuji, X. Li, M. Caricato, A. V. Marenich, J. Bloino, B. G. Janesko, R. Gomperts, B. Mennucci, H. P. Hratchian, J. V. Ortiz, A. F. Izmaylov, J. L. Sonnenberg, D. Williams-Young, F. Ding, F. Lipparini, F. Egidi, J. Goings, B. Peng, A. Petrone, T. Henderson, D. Ranasinghe, V. G. Zakrzewski, J. Gao, N. Rega, G. Zheng, W. Liang, M. Hada, M. Ehara, K. Toyota, R. Fukuda, J. Hasegawa, M. Ishida, T. Nakajima, Y. Honda, O. Kitao, H. Nakai, T. Vreven, K. Throssell, J. A. Montgomery, Jr., J. E. Peralta, F. Ogliaro, M. J. Bearpark, J. J. Heyd, E. N. Brothers, K. N. Kudin, V. N. Staroverov, T. A. Keith, R. Kobayashi, J. Normand, K. Raghavachari, A. P. Rendell, J. C. Burant, S. S. Iyengar, J. Tomasi, M. Cossi, J. M. Millam, M. Klene, C. Adamo, R. Cammi, J. W. Ochterski, R. L. Martin, K. Morokuma, O. Farkas, J. B. Foresman, and D. J. Fox, Gaussian 16, Revision C.01, Gaussian, Inc., Wallingford CT, 2019.
[27] R. Dennington, T.A. Keith, J.M. Millam, GaussView 5.0.8, Semichem Inc. Shawnee Mission KS, 2008.
[28] J. Tomasi, B. Mennucci, R. Cammi, Chem. Rev. 105 (2005) 2999.
[29] A.D. Becke, Phys. Rev. A 38 (1988) 3098.
[30] C. Lee, W. Yang, R.G. Parr, Phys. Rev. B 37 (1988) 785.
[31] S.F. Boys, F. Bernardi, Mol. Phys. 19 (1970) 553.
[32] D.A. Case, V. Babin, J. Berryman, R.M. Betz, Q. Cai, D.S. Cerutti, T. Cheatham, T. Darden, R. Duke, H. Gohlke, A. Götz, S. Gusarov, N. Homeyer, P. Janowski, J. Kaus, I. Kolossváry, A. Kovalenko, T.-S. Lee, P.A. Kollman, AMBER 14, University of California, San Francisco, 2014.
[33] C.I. Bayly, P. Cieplak, W. Cornell, P.A. Kollman, J. Phys. Chem. 97 (1993) 10269.
[34] E. Vanquelef, S. Simon, G. Marquant, E. Garcia, G. Klimerak, J.C. Delepine, P. Cieplak, F.-Y. Dupradeau, Nucl. Acids Res. 39 (2011) W511.
[35] F.-Y. Dupradeau, A. Pigache, T. Zaffran, C. Savineau, R. Lelong, N. Grivel, D. Lelong, W. Rosanski, P. Cieplak, Phys. Chem. Chem. Phys. 12 (2010) 7821.
[36] P. Bouř, xshell, Acad. Sci.: Prague (2009–2022).
[37] P. Bouř, rdf, Acad. Sci.: Prague (2008–2022).
[38] N.I.o.S.a. Technology, 2013 (https://cccbdb.nist.gov/vibscalejust.asp - accessed in 2022).
[39] V. Andrushchenko, D. Tsankov, M. Krasteva, H. Wieser, P. Bouř, J. Am. Chem. Soc. 133 (2011) 15055.
[40] V. Andrushchenko, L. Benda, O. Páv, M. Dračínský, P. Bouř, J. Phys. Chem. B 119 (2015) 10682.
[41] Y. Kond, H. Takahashi, M. Onda, Chem. Pharm. Bull. 33 (1985) 1083.
[42] T.A. Oster, T.M. Harris, J. Org. Chem. 48 (1983) 4307.
[43] V. Jäger, M. Frey, Liebigs Ann. Chem. 1982 (1982) 817.
[44] B. Edwin, I.H. Joe, Spectrochim. Acta A Mol. Biomol. Spectrosc. 114 (2013) 633.